Astron. Astrophys. 356, 315–318 (2000)

ASTRONOMY AND ASTROPHYSICS

An estimation of the shape and temporal variation of the solar wind sonic, Alfvénic and fast magnetosonic surfaces

G. Exarhos and X. Moussas

Section of Astrophysics, Astronomy and Mechanics, Physics Department, National University of Athens, Panepistimiopolis GR 15783, Zografos, Athens, Greece

Received 10 March 1999 / Accepted 27 January 2000

Abstract. In this work we find the shape and dimension of the solar wind transition surfaces, namely the slow (sonic), the fast magnetosonic and the Alfvén surface, as a function of heliospheric latitude using actual experimental data from *Ulysses* spacecraft during its first pole to pole journey. We also give the temporal variation of the radius of these surfaces using measurements from spacecraft at 1 AU. All transition surfaces are equatorial elongated. The sonic surface is the most asymmetric surface with polar radius $\sim 1.5R_\odot$ and equatorial radius $\sim 2R_\odot$. The Alfvén and the fast magnetosonic surfaces seems to be less asymmetric. The Alfvén polar and equatorial radius is $\sim 14R_\odot$ and $\sim 17R_\odot$ respectively while the fast magnetosonic polar and equatorial radius is $\sim 15R_\odot$ and $\sim 18R_\odot$ respectively. The temporal variation of the transition surfaces radii follows the 11-year solar cycle except for the sonic radius which seems not to vary remarkably with time.

Key words: hydrodynamics – Sun: solar wind

1. Introduction

The problem of the various astrophysical flows and wind acceleration has been studied by many researchers (Parker 1958; Weber & Davis 1967; Habbal & Tsinganos 1983; Heyvaerts & Norman, 1996; MacGregor 1996; Trussoni et al. 1996; Tsinganos et al. 1996, and references therein) under hydrodynamic or magnetohydrodynamic approximations.

The MHD approximation leads to differential equations which appear singularities or critical points (Tsinganos et al. 1996). On the other hand there are purely HD models (Tsinganos & Trussoni 1990; Lima & Priest 1993; Kakouris & Moussas 1996) where the differential equations do not possess critical points. In these models the characteristic transitions surfaces (i.e. the transition of the flow speed to the fast magnetosonic speed) is not critical surfaces.

Our work is to estimate the shape and location of the transition surfaces of the solar wind flow in the case where there are no singularities. For the purpose of our work we use the model of Lima & Priest (1993) which is a purely hydrodynamic model with no singular points.

The position of a transition surface is determined by setting the flow speed equal to the corresponding characteristic speed (i.e. the speed of sound c_s for the sonic surface, the Alfvén speed u_A for the Alfvén surface and the fast magnetosonic speed u_{ms} for the fast magnetosonic surface). In this work we define the radius of a transition surface as the distance where the radial component of the solar wind velocity equals the radial component of the characteristic velocity.

2. The transition surfaces

To calculate the shape and the location of the transition surfaces we need to know the dependence of the solar wind parameters with the radial distance and the heliolatitude. We apply for this purpose the model of Lima & Priest (1993) modified for the case of the solar wind. The flow velocity and density are given by the relationships

$$\bar{V_r}(R,\theta) = Y(R)\upsilon_r(\theta) \tag{1}$$

$$\bar{\rho}(R,\theta) = \frac{g(\theta)}{Y(R)R^2} \tag{2}$$

where $\bar{V_r} = \frac{V_r}{V_o}$, $\bar{\rho} = \frac{\rho}{\rho_o}$ and $R = \frac{r}{r_o}$. The subscript "o" denotes the value at the reference distance r_o. The functions $\upsilon_r(\theta)$ and $g(\theta)$ are given by

$$\upsilon_r(\theta) = \sqrt{\frac{1+\mu sin^{2\epsilon}\theta}{1+\omega sin^{2\epsilon}\theta}} \tag{3}$$

$$g(\theta) = 1 + \omega sin^{2\epsilon}\theta. \tag{4}$$

The function $Y(R)$ satisfies the differential equation

$$\frac{dY}{dR} = \frac{Y}{R}\left[\frac{\epsilon\omega\nu^2 R - 2(\epsilon+2)\lambda^2}{\lambda^2 - 2\mu\epsilon Y^2 R^2}\right] \tag{5}$$

with $R \geq 1$ and $Y(1) = 1$ where μ, ϵ, λ, ω and ν are the model parameters (see Lima & Priest 1993). For the solar wind conditions during the time period from mid-1994 till the end of 1995, the values of these parameters are (Lima & Tsinganos 1996)

$\mu = -0.44$, $\epsilon = 4$, $\omega = 0.72$, $\nu = 120$ and $\lambda = 0.5$.

Send offprint requests to: X. Moussas

Based on these values we find that $\epsilon\omega\nu^2 \gg 2(\epsilon+2)\lambda^2$ and $2|\mu|\epsilon \gg \lambda^2$. So in a very good approximation the differential Eq. (5) takes the form

$$\frac{dY}{dR} = -\frac{\omega\nu^2}{2\mu Y R^2} \tag{6}$$

which is a first order differential equation and its solution is

$$Y(R) = \sqrt{1 - \frac{\omega\nu^2}{\mu}(1 - \frac{1}{R})}. \tag{7}$$

2.1. The sonic surface

The sonic surface is defined as the surface where the solar wind velocity V_r equals the speed of sound c_s

$$V_r(R_s) = c_s(R_s) \tag{8}$$

where R_s is the sonic surface radius. The speed of the sound is defined as

$$c_s^2 = \Gamma\frac{p}{\rho} \tag{9}$$

where $\Gamma = 5/3$ the specific heats ratio for monoatomic gas.

The pressure p, following the model of Lima & Priest (1993), is given by the expression

$$p = Q(R,\theta)\rho_o V_o^2/2 \tag{10}$$

where the function $Q(R,\theta)$ has the form

$$Q(R,\theta) = Q_o(R) + Q_1(R)\frac{sin^{2\epsilon}\theta}{\epsilon}. \tag{11}$$

The functions $Q_o(R)$ and $Q_1(R)$ satisfy the equations

$$Q_1(R) = \frac{\lambda^2}{YR^4} \tag{12}$$

$$\frac{dQ_o}{dR} + \frac{\nu^2}{YR^4} + \frac{2}{R^2}\frac{dY}{dR} = 0. \tag{13}$$

We note that for the case of the solar wind the function $Q_1(R)$ is much smaller than the function $Q_o(R)$, so we can ignore it.

If we combine now Eq. (7) and Eq. (13) we find that

$$\frac{dQ_o}{dR} = -\frac{\nu^2}{YR^4}(1 - \frac{\omega}{\mu}) \tag{14}$$

which we solve numerically using the Ulysses measurements. The solar wind pressure is expressed now by the relationship

$$p = Q_o(R)\rho_o V_o^2/2 \tag{15}$$

and it is only a function of the radial distance R, not of the polar angle θ. Finally the sonic radius R_s is calculated from the Eq. (8) in combination with the Eqs. (15), (2) and (9)

$$\frac{2Y(R_s)}{\Gamma Q_o(R_s)R_s^2}(1 + \mu sin^{2\epsilon}\theta) = 1. \tag{16}$$

In Fig. 1 we give the shape and the location of the sonic surface. We see that the sonic surface is equatorial elongated with equatorial radius $\sim 2R_\odot$ and polar radius $\sim 1.5R_\odot$. So we can conclude that the fast solar wind emanating from the coronal holes has a smaller sonic radius than the slow solar wind.

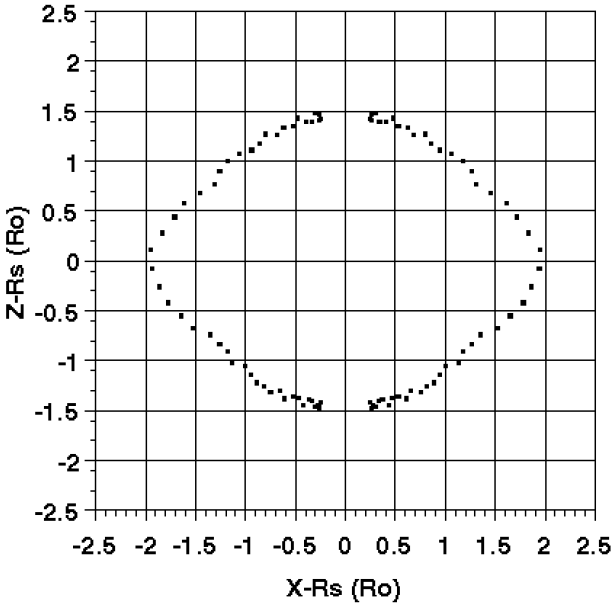

Fig. 1. The shape of the sonic surface based on measurements of Ulysses spacecraft during its first pole to pole journey.

2.2. The Alfvén surface

We define the Alfvén surface as the surface where the solar wind radial velocity V_r equals the radial Alfvén velocity u_A which is given by the relationship

$$u_A^2 = \frac{B_r^2}{\mu_o\rho} \tag{17}$$

where B_r is the radial component of the heliospheric magnetic field. So we have

$$V_r(R_A) = u_A(R_A) \tag{18}$$

where R_A is the Alfvén radius. We assume that $B_r = B_{r_o}(r_o/r)^2$, so from Eq. (2) and Eq. (1) we find

$$V_o^2 Y^2(R_A)\upsilon_r^2(\theta) = \frac{B_r^2(R_A)}{\mu_o\rho_o\frac{g(\theta)}{Y(R_A)R_A^2}}. \tag{19}$$

If we express the parameters V_o and ρ_o as a function of the corresponding parameters that Ulysses measures we take

$$V_o = \frac{V_r(R_U,\theta)}{Y(R_U)\upsilon_r(\theta)} \tag{20}$$

$$\rho_o = \frac{\rho(R_U,\theta)Y(R_U)R_U^2}{g(\theta)}. \tag{21}$$

Then Eq. (19) with the help of Eq. (20) and Eq. (21) gives

$$Y(R_A)R_A^2 = \frac{B_r^2(R_U,\theta)R_U^2 Y(R_U)}{\mu_o g(\theta)\rho(R_U,\theta)V_r^2(R_U,\theta)} \tag{22}$$

where the subscript "U" denotes the value of each parameter measured by Ulysses. In Fig. 2 we give the shape and the location of the Alfvén surface. We see that the Alfvén surface is less elongated at the equator than the sonic surface. The equatorial radius is $\sim 17R_\odot$ while the polar radius is $\sim 14R_\odot$.

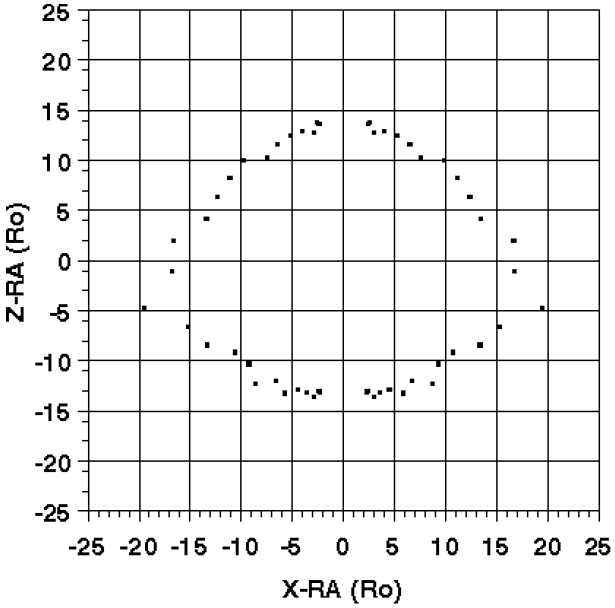

Fig. 2. The shape of the Alfvén surface based on measurements of Ulysses spacecraft during its first pole to pole journey.

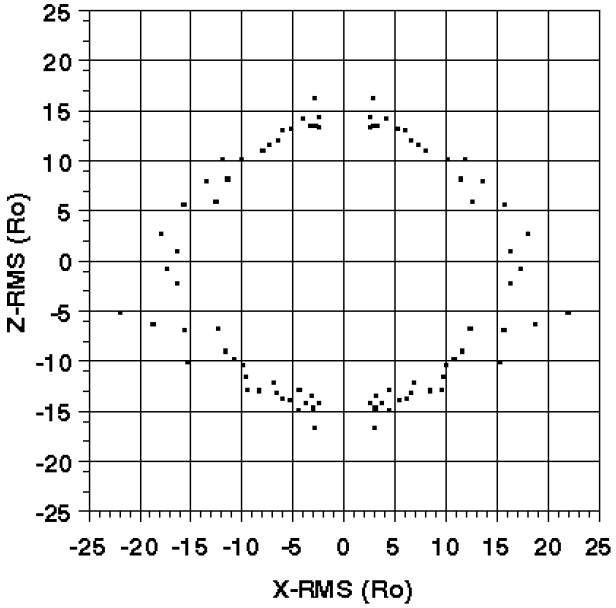

Fig. 3. The shape of the magnetosonic surface based on measurements of Ulysses spacecraft during its first pole to pole journey.

2.3. The magnetosonic surface

The Magnetosonic surface is defined as the surface where the solar wind radial velocity V_r equals the radial magnetosonic velocity u_{ms} which is given by the relationship

$$u_{ms}^2 = c_s^2 + u_A^2 = \Gamma \frac{p}{\rho} + \frac{B_r^2}{\mu_o \rho}. \quad (23)$$

So in a distance equal to R_{ms} we have

$$V_r(R_{ms}) = u_{ms}(R_{ms}). \quad (24)$$

From Eq. (1), Eq. (2), Eq. (11), Eq. (20), Eq. (21) and Eq. (24) we find

$$V_r^2(R_U,\theta) = \left[\frac{B_r^2(\frac{R_U}{R_{ms}})^2}{\mu_o \rho(R_U,\theta)} + \right.$$
$$\left. + \frac{\frac{\Gamma\, p(R_U,\theta)}{\rho(R_U,\theta)} Q(R_{ms}) R_{ms}^2}{Q(R_U) R_U^2} \right] \frac{Y(R_U)}{Y(R_{ms})}. \quad (25)$$

In Fig. 3 we give the shape and the location of the magnetosonic surface. The similarity with the Alfvén surface is obvious. The equatorial radius of the magnetosonic surface is $\sim 18 R_\odot$ while the polar radius is $\sim 15 R_\odot$.

3. Time variation of the radius of the transition surfaces

The radius of the transition surfaces apart from the latitude variation experiences also time variations as a consequence of the solar wind velocity, density and magnetic field variations due to solar activity. Using continuous measurements from different spacecraft at 1 AU (OMNI database) since 1963 we can calculate the transition radii as a function of time. From Eq. (16), Eq. (22) and Eq. (25) and the time series of 1 AU measurements we take the transition radii time dependence which is shown in Fig. 4.

The temporal variation of the Alfvén and magnetosonic radius follows more or less the 11-year variation of the sunspot number. They double their size from solar minimum to solar maximum. This situation is valid for the region near the ecliptic plane for which we have direct measurements since 1963. For high latitude regions we do not have direct measurements for such a long time period and we cannot extent the previous result into this region. We have to wait for *Ulysses* second pole to pole journey which will occur during a period of solar maximum activity. Then we can compare the results with those obtained during the first pole to pole journey which occurred during a period of solar minumum activity, although for solar maximum activity conditions we expect more spherical shapes for these surfaces.

The sonic surface seems not to be affected by the solar activity and shows a characteristic stability. Its radius does not vary more than $0.005 R_\odot$ according to our computations. For higher latitudes this situation may not be true. We expect a temporal variation in the radius of the sonic surface with the heliospheric latitude due to changes in the size of the coronal holes.

4. Conclusions

We have calculated the shape and the location of the transition surfaces, namely the sonic, the Alfvén and the fast magnetosonic surface, using Ulysses measurements at different heliospheric latitudes. The results show that all surfaces is equatorial elongated but the Alfvén and fast magnetosonic surface have a more spherically symmetric shape. Our results are based on the hydrodynamic model of Lima & Priest (1993), modified for the case of the solar wind.

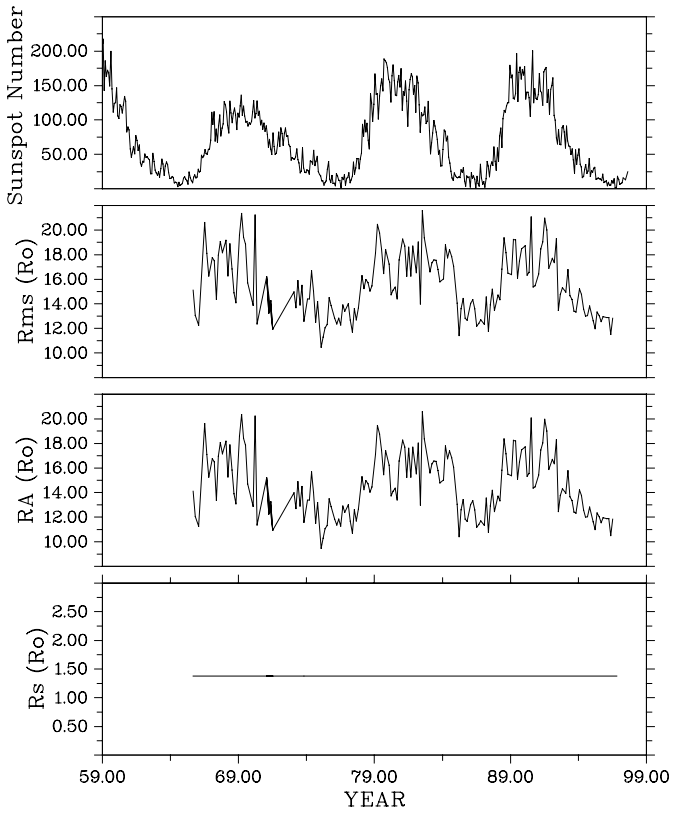

Fig. 4. Temporal variation of transition radii (R_s*: sonic,* R_A*: Alfvén and* R_{ms}*: magnetosonic*) based on in-ecliptic measurements at 1 AU. The sunspot number is presented as an index of solar activity.

The temporal variations of the Alfvén and magnetosonic radius, as they are calculated using in-ecliptic measurements at 1 AU, follow the variations of solar activity. Their radii double their size near solar maximum activity from the corresponding values near solar minimum activity. The sonic radius does not seem to be affected by the solar activity.

Acknowledgements. We thank the University of Athens for the Grant 70/4/2469 for Space Physics. We are indebted to the referee for his help in improving this paper. We also thank NSSDC, the investigators of all spacecraft experiments which have contributed to the OMNI database (IMP, HEOS 1 and 2, etc.) and especially Dr J. King for the excellent organization of the data center. G. Exarhos is grateful to the Greek State Scholarship Foundation (S.S.F.: I.K.Y.) for his scholarship.

References

Habbal S.R., Tsinganos K., 1983, J. Geophys. Res. 88, 1965
Heyvaerts J., Norman, C.A., 1996, In: Tsinganos K. (ed.) Solar and Astrophysical MHD flows, Kluwer, Dordrecht, p. 459
Kakouris A., Moussas X., 1996, A&A 306, 537
Lima J.J.G., Priest E.R., 1993, A&A 268, 641
Lima J., Tsinganos K. 1996, Geophys. Res. Lett. 23, 117
MacGregor K., 1996, In: Tsinganos K. (ed.) Solar and Astrophysical MHD flows, Kluwer, Dordrecht, p. 301
Parker E.N., 1958, Phys. Rev. 110, 1445
Trussoni E., Sauty C., Tsinganos K., 1996, Tsinganos K. (ed.) In: Solar and Astrophysical MHD flows, Kluwer, Dordrecht, p. 383
Tsinganos K., Trussoni E., 1990, A&A 231, 270
Tsinganos K., Sauty E., Surlantzis G., et al., 1996, MNRAS 283, 811
Weber E.J., Davis Jr., L, 1967, ApJ 148, 217